Nanoscale Advances

ROYAL SOCIETY OF CHEMISTRY

PAPER

View Article Online
View Journal | View Issue



Cite this: *Nanoscale Adv.*, 2025, **7**, 7570

# Boosting the electrical properties of nano-structured ($Ga_{10}Se_{90}$)-MWCNT bilayer thin films

Aarif Hussain Wani,[a] Shakeel Ahmad Khandy, *[b] Mandeep Singh*[a] and Shabir Ahmad*[a]

Selenium-based chalcogenide semiconductors are of growing interest for optoelectronic applications due to their high DC conductivity, photoconductivity, and carrier mobility. In this work, $Ga_{10}Se_{90}$-MWCNT nanocomposite thin films were fabricated *via* thermal evaporation and subsequently modified using swift heavy ion (SHI) irradiation using 70 MeV $Ni^{7+}$ ions at fluences of $1 \times 10^{12}$ to $1 \times 10^{13}$ ions per $cm^2$. SHI irradiation promoted the homogeneous mixing of CNTs within the GaSe matrix, enhancing the electrical properties through defect engineering and interfacial charge transfer. Characterization *via* FESEM, EDX, and FTIR confirmed uniform nanoparticle dispersion and strong GaSe-CNT interactions. Post-irradiation, DC conductivity increased from $2.11 \times 10^{-4}$ to $2.97 \times 10^{-3}$ $\Omega^{-1}$ $cm^{-1}$, photoconductivity from $5.16 \times 10^{-5}$ to $2.90 \times 10^{-3}$ $\Omega^{-1}$ $cm^{-1}$, and carrier mobility from 50.9 to 475.1 $cm^2$ $V^{-1}$ $s^{-1}$. These enhancements are attributed to improved charge transport *via* CNT networks and SHI-induced acceptor states. The results highlight the tunability of GaSe-CNT composites *via* SHI, supporting their potential use in advanced optoelectronic devices.

Received 26th June 2025
Accepted 26th September 2025

DOI: 10.1039/d5na00626k

rsc.li/nanoscale-advances



## 1 Introduction

Chalcogenides are versatile semiconducting materials, and the electrical properties of chalcogenide-based semiconductors are significant for a variety of electronic and optoelectronic applications. Their physical properties can be tailored by engineering their composition. Electrical conductivity is influenced by several factors, including the chalcogenide's composition and doping levels. They have attracted interest worldwide because of their unique optical and electrical properties, corresponding to a wide range of applications such as in energy storage devices, communication, photoconductors,[1] phase change memory devices,[2] photovoltaics, photodiodes, *etc.*[3,4] It has been demonstrated that incorporating doping elements in chalcogenide glasses can lead to significant modification of their physical properties. There are various techniques available for the deposition of thin films of chalcogenides such as chemical vapor deposition (CVD), chemical bath deposition (CBD), sol–gel synthesis, solvothermal techniques, pulsed laser deposition, *etc.* Thermal evaporation is one of the easiest and most cost-effective techniques for the deposition of thin films.[5,6] Gallium selenide (GaSe), a layered semiconductor monochalcogenide, due to its composition dependent properties has emerged as a vital semiconducting material in the fields of photonics and optoelectronics. It has a hexagonal structure, and finds various applications due to its novel optoelectronic properties.[7,8] Each individual layer of gallium selenide is made up of two sheets of Ga ions in the middle and two sheets of Se ions on the top and bottom. Similar to other layered 2D structures like graphene, adjacent GaSe layers are bound by weak van der Waals forces, which allows for the structure to be peeled off by mechanical or liquid exfoliation.[9] The ultra-thin few or single layer 2D gallium selenide nanosheets or nanoparticles that are produced have a wide range of applications, including in integrated optics, optical information communications, *etc.*[10–12] In layered gallium chalcogenide semiconductor crystal materials such as GaSe, GaS, and GaTe, free excitons play a vital role in optical, photoconductivity and luminescence properties. The exciton states have densities that are higher than those at the edges of the valence and conduction bands; the exciton maximum can be seen in the measured values of photoluminescence, absorption, reflection, and photoconductivity spectra. With a pseudo direct bandgap of the order of 2.1 eV and thickness dependent opto-electronic properties, GaSe has emerged as a promising candidate for the implementation of thin film transistors (TFTs), photodetectors and photoconductors with fast response and high sensitivity. GaSe, exhibiting novel optoelectronic properties, is a promising material for photoconductor and nonlinear optical applications. Non-linear optical materials are used in the frequency conversion of laser light.[13,14] A photoconductor is a light-sensitive component, used in a printer or copier that creates

[a]*Department of Physics, Islamic University of Science and Technology, Awantipora, Kashmir-192122, India. E-mail: mandeep@iust.ac.in; shabir.ahmad@iust.ac.in*
[b]*Frontier Research Institute of Interdisciplinary Sciences, Islamic University of Science and Technology, Awantipora, Kashmir-192122, India. E-mail: shakeelkhandy11@gmail.com*

images using electrical properties. Gallium selenide (GaSe), due to its high photoconductivity values, can be applied as a photoconductor.[13] However, the photoconductivity values of GaSe ($\sim 10^{-5}$ $\Omega^{-1}$ $cm^{-1}$) are relatively not large, and photoconductors should exhibit high mobility of charge carriers, while GaSe has low mobility values of the order of 0.6–200 $cm^2$ $V^{-1}$ $s^{-1}$,[15] limiting its application as a photoconductor. The mobility and electrical conductivity of the bilayer thin film of GaSe can be enhanced to reasonable levels by incorporating small amounts of CNTs into the matrix layers of GaSe.[16,17] Carbon nanotubes (CNTs) are versatile nanomaterials. Given their potential to exhibit unique physical properties, their incorporation with other materials could have an impact on a wide range of scientific and technological fields, and they have attracted the attention of researchers worldwide. Currently, there is a lot of interest worldwide in CNTs. Due to their novel properties such as high electrical conductivity, high mechanical strength, light weight, high mobility, *etc.*, their incorporation with other materials could lead to enhancement in their properties.[18] From literature studies, a few studies reported that doping CNTs in selenium in bulk form resulted in the enhancement of optoelectronic properties. Researchers found that there is a significant change in the electronic structure, potentially narrowing or widening the band gap. CNT doping could potentially lead to an enhancement in electrical conductivity and mobility of charge carriers, depending on the doping concentration and the interaction between CNTs and the chalcogenide matrix. CNTs, due to their high mechanical strength, could result in increased durability and flexibility upon their incorporation with other materials,.[19–21] This work reports the effect of doping of MWCNTs on the electrical properties of a gallium-selenide $Ga_{10}Se_{90}$ nanocomposite material in thin film form, followed by SHI irradiation for tailoring the electrical properties of the prepared thin films. From this analysis, we reported a substantial improvement in the electrical conductivity and mobility of the $Ga_{10}Se_{90}$ crystal material after incorporation of MWCNTs. The homogeneous mixing of $Ga_{10}Se_{90}$ nanoparticles into the matrix layers of MWCNTs is achieved by SHI irradiation of 70 MeV of $Ni^{7+}$ ions. The use of swift heavy ion irradiation (SHI) can be beneficial in many ways such as for modification of the properties of thin films, surfaces of bulk solids, *etc.* It could lead to defect formation, amorphization and homogeneous mixing of the material along the projectile ion beam. The SHI ion beam penetrates deep inside the material and creates a narrow disorder zone along its trajectory. When an ion beam penetrates through a material, its energy is lost mainly through two processes: (i) nuclear energy loss due to elastic collision with the atoms of the solid, dominating at low energies of the order of a few keV. (ii) Electronic energy loss due to inelastic collisions with atomic electrons, which dominates at large energy of the order of MeV such as for SHI irradiation. The electronic energy loss from SHI irradiation causes disruption of the crystal lattice leading to homogeneous mixing of the composite material and increasing the concentration of the charge carriers, resulting in improved conductivity of the investigated material. The energy is transferred from the ion projectile to the atoms through excitation and ionization of surrounding electrons and electronic excitation is generated, which is transferred to the lattice atoms, producing ion tracks, which can be understood using the Coulomb explosion model and thermal spike models.[22] The Coulomb explosion model is attributed to electrostatic repulsion between positively charged ions causing the disruption of the material's structure leading to amorphisation and exceptional changes in electrical properties of the investigated material. According to the thermal spikes model, when SHI irradiation passes through a material, it deposits a huge amount of energy in a very small cylindrical region (with a radius of a few nanometers). This creates a localized ultra-fast 'thermal spike', an abrupt and intense rise in temperature of the electronic system (thousands of kelvins) in a few femtoseconds to picoseconds. The hot electrons then transfer energy to the lattice *via* electron-phonon coupling, causing amorphisation of the material, followed by quenching, potentially leading to uniform distribution of CNTs into the matrix layers of GaSe. The rapid heating and quenching leads to defect formation. Such defects can act as donors or acceptors, effectively increasing the free carrier concentration, thereby enhancing the electrical properties of the investigated material.[21,23] SEM confirms the morphology of the as-prepared ($Ga_{10}Se_{90}$)-MWCNT composite material. From SEM micrographs (Fig. 1(c)–(f)), it is clearly seen that the CNTs are uniformly distributed into GaSe matrix layers post SHI irradiation. EDX confirms the elemental composition, and it can be seen from Fig. 1(a) and (b) that the intense peaks of CNTs are observed post SHI irradiation. Conductivity measurements were carried out using the well-known van der Pauw four probe method. The dark DC current and photocurrent were measured with the help of a picometer (pm). The estimated measurements of conductivity show an appreciable improvement in both the DC conductivity and photoconductivity of the as-prepared thin film and SHI-irradiated thin films of ($Ga_{10}Se_{90}$)-MWCNT. From Fig. 3, it can be seen that there is an appreciable increase in the electrical conductivity of SHI-irradiated GaSe-CNT thin films TF2, TF3, and TF4 compared to the as-prepared (un-irradiated) thin film TF1. Mobility studies were carried out using the Hall effect. Zishan H Khan *et al.*'s investigation on $Ga_xSe_{100-x}$ ($x = 3$, 6, 9, 12)[24] reported conductivity in the range of $10^{-10}$ to $10^{-8}$ $\Omega^{-1}$ $cm^{-1}$.[24] Hana Khan *et al.*'s investigation on a CNT modified $Ga_{10}Se_{90}$ composite reported conductivity in the range of $10^{-4}$ $\Omega^{-1}$ $cm^{-1}$.[25] The current investigation of the $Ga_{10}Se_{90}$-MWCNT composite reported an appreciable enhancement in the conductivity and mobility of the prepared thin films post SHI irradiation. The DC conductivity is increased from $2.11 \times 10^{-4}$ $\Omega^{-1}$ $cm^{-1}$ (TF1 unirradiated) to $2.97 \times 10^{-3}$ $\Omega^{-1}$ $cm^{-1}$ (TF4, SHI-irradiated thin film), while the photoconductivity increased from $5.16 \times 10^{-5}$ $\Omega^{-1}$ $cm^{-1}$ to $2.90 \times 10^{-3}$ $\Omega^{-1}$ $cm^{-1}$ at a temperature of 352.4 K and the mobility increased from 50.99 $cm^2$ $V^{-1}$ $s^{-1}$ (unirradiated TF1) to 475.1 $cm^2$ $V^{-1}$ $s^{-1}$ (SHI-irradiated TF4 thin film), suggesting the investigated composite material as a promising candidate for broader optoelectronic applications.

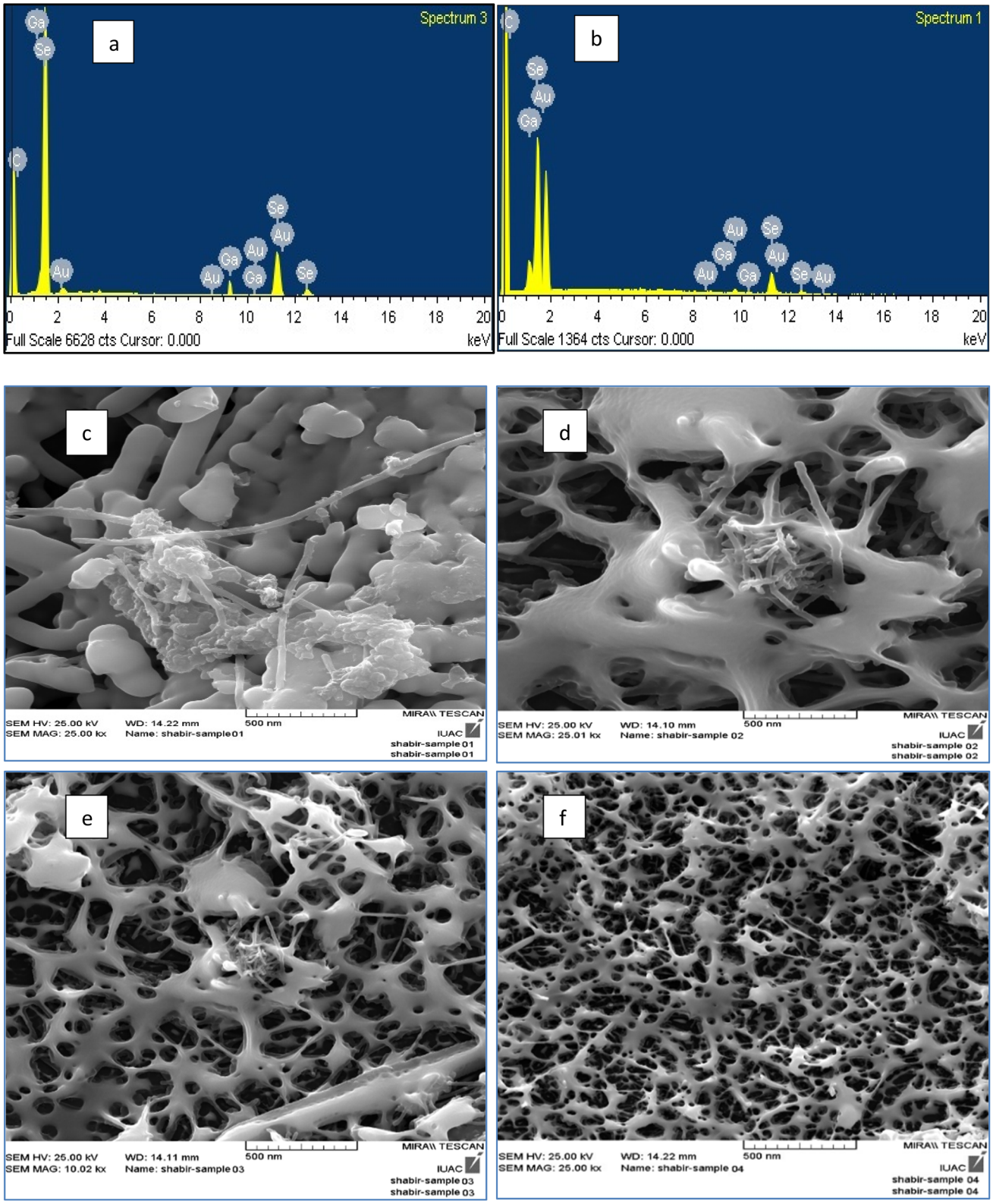


Fig. 1 EDX and SEM micrographs of the as-prepared and SHI-irradiated thin films. (a) The EDX spectrum of the unirradiated ($Ga_{10}Se_{90}$)-MWCNT bilayer thin film; (b) the EDX spectrum of the $1 \times 10^{13}$ ions per $cm^2$-irradiated ($Ga_{10}Se_{90}$)-MWCNT bilayer thin film; (c) an SEM image of the as-prepared ($Ga_{10}Se_{90}$)-CNT bilayer thin film; (d) an SEM image of the $1 \times 10^{12}$ ions per $cm^2$-irradiated thin film; (e) an SEM image of the $5 \times 10^{12}$ ions per $cm^2$-irradiated thin film; and (f) an SEM image of the $1 \times 10^{13}$ ions per $cm^2$-irradiated thin film.

## 2 Experimental studies

A homogeneous mixture of $Ga_{10}Se_{90}$ was prepared using a solid state reaction technique with 3N elemental purity *via* thermal evaporation. The quantities of Ga and Se were weighed through the electronic balance method (least count of $10^{-4}$ g) in accordance with their atomic weight percentages. A quartz ampoule containing 4.5 g of finely powdered gallium selenide was sealed under a $10^{-6}$ Torr vacuum. The sealed ampule was heated steadily at a rate of 5 °C $min^{-1}$ up to 950 °C inside a microprocessor-controlled programmable muffle furnace. The material inside the ampoule is left to melt at 950 °C for 15 hours. The resulting melt of $Ga_{10}Se_{90}$ was rapidly quenched in ice-cooled water after 15 hours. The ampoule was then broken down and the obtained ingot of $Ga_{10}Se_{90}$ is ground into a fine powder with the help of a pestle and mortar. MWCNTs (0.05 mg) with a diameter of 20–40 nm and a length of several micrometers were dissolved in 5 mL of dimethylformamide (DMF) solution and ultrasonically aged for 8 hours. The glass substrates were well cleaned by using an ultrasonic cleaner with acetone for 5–10 minutes. The spin coating method with 2000 rpm was used to deposit a MWCNT thin-film of approximately 300 nm thickness on a cleaned glass substrate. The $Ga_{10}Se_{90}$ sample is loaded on a molybdenum boat under a vacuum of $10^{-5}$ Torr and an electric current is passed through the heating element, which heats up due to the resistance of the material. The temperature of the boat increases, and as a result the material in the boat starts to melt and then vaporize. A thin layer of $Ga_{10}Se_{90}$ of about 300 nm was formed above the MWCNT layer *via* thermal evaporation. The rigorous homogeneous mixing of the bilayer thin film of the ($Ga_{10}Se_{90}$)-CNT nanocomposite formed is achieved by SHI irradiation using 70 MeV nickel ($Ni^{7+}$) ions in the fluence range of $1 \times 10^{12}$ to $1 \times 10^{13}$ ions per $cm^2$ using the 15UD Pelletron Accelerator facility at IUAC, New Delhi, India, for tailoring the electrical properties. A 1 pnA (particles nanoampere) beam current was used to scan an area of 1 $cm^2$. The electronic loss ($S_e$) was 21.670 eV $nm^{-1}$, nuclear energy loss ($S_n$) was 0.059 eV $nm^{-1}$, and projectile range was 15.31, which is a feasible range for ions to traverse the entire film thickness. Four thin films of the ($Ga_{10}Se_{90}$)-MWCNT nanocomposite, labeled as TF1, TF2, TF3 and TF4, were prepared. TF1 is the as-prepared thin film of ($Ga_{10}Se_{90}$)-MWCNT, not exposed to any SHI irradiation. The other three bilayer thin films, TF2, TF3, and TF4, are exposed to the SHI irradiation of 70 MeV $Ni^{7+}$ ions with fluence of $1 \times 10^{12}$ ions per $cm^2$, $5 \times 10^{12}$ ions per $cm^2$ and $1 \times 10^{13}$ ions per $cm^2$, respectively. The film thickness is measured using the ellipsometry technique. Compositional analysis and surface studies were carried out by using energy dispersive X-ray (EDX) analysis and field emission scanning electron microscopy (FESEM) (model: Sigma by Carl Zeiss employed with a Gemini Column patented technology of Corl Zeiss). Silver paste was applied to the thin films to create an electrode with a 1 mm gap for electrical tests. The thin film was mounted in a specially made metallic sample holder with a transparent window that let in white light from a 200 W tungsten lamp for measurements of photoconductivity in the temperature range of 310–390 K at a constant voltage of 1.5 V. For measurements of dark DC conductivity, the same parameters were used. Due to the lamp's extremely low temperature (almost 2–4 K), the thermal impacts it produces are not particularly noticeable. A digital luxmeter 3650 lx (MS6610) was used to measure the lamp's intensity. The mobility values of the as-prepared and SHI-irradiated thin films is estimated with the help of the Hall effect (van der Pauw's method). The measurements were carried out at room temperature (300 K) and a magnetic field intensity of 0.570 Tesla.

## 3 Results and discussion

### 3.1 EDX and SEM characterization

The elemental composition of the investigated thin films is confirmed with the help of energy dispersive X-ray analysis (EDX), a widely used technique. The EDX micrographs of the investigated thin films are shown in Fig. 1(a) and (b). From the EDX micrograph, Fig. 1(a), of the un-irradiated TF1, less intense peaks of CNTs are observed, while the EDX micrograph of the SHI-irradiated TF4 shows highly intense peaks of both CNTs and Ga-Se confirming the uniform distribution of the composite post SHI irradiation. The Au peaks arise due to the electrodes of Au being used for conduction of electric current in the as-prepared thin films. Surface micrographs clearly depicted the incorporation of $Ga_{10}Se_{90}$ nanoparticles on the surface of CNT nanotubes. SEM confirms the surface morphology of the investigated material. The SEM micrographs of the prepared composite bilayer thin films are shown in Fig. 1(c) to Fig. 1(f). The SEM micrograph of the un-irradiated TF1 thin film (Fig. 1(c)) shows agglomeration of Ga-Se particles on the surface of the CNTs, and the SEM micrograph of the TF2 thin film (Fig. 1(d)) shows agglomeration of CNTs into the Ga-Se matrix. The SEM micrographs of the TF3 and TF4 thin films with high fluence (Fig. 1(e), and (f)) show uniform distribution of Ga-Se nanoparticles into the matrix layers of the CNTs. This is attributed to the fact that upon SHI irradiation, the size of the Ga-Se nanoparticles decreases, and they are uniformly incorporated in the matrix layers of MWCNTs. With the increasing fluence of SHI irradiation, more and more particles are incorporated into the GaSe matrix layers, thereby increasing the uniform distribution of CNTs into GaSe matrix layers. From the surface morphology, it is clearly found that appreciable homogeneous mixing is achieved in the SHI-irradiated TF4 thin film with high fluence (see Fig. 1(f)). The CNTs, due to their highly conductive behavior, form conductive channels within Ga-Se matrix layers, resulting in enhanced electrical properties of the investigated material.

### 3.2 FTIR analysis

The Fourier transform infrared spectra of the as-prepared and SHI-irradiated samples are shown in Fig. 2. The spectra show vibrational phonon modes with different intensities. The low wavenumber peaks between 1200 $cm^{-1}$ and 500 $cm^{-1}$ are attributed to stretching and bending modes of $Ga_{10}Se_{90}$. The high intensity peak around 1130 $cm^{-1}$ may be related to high-

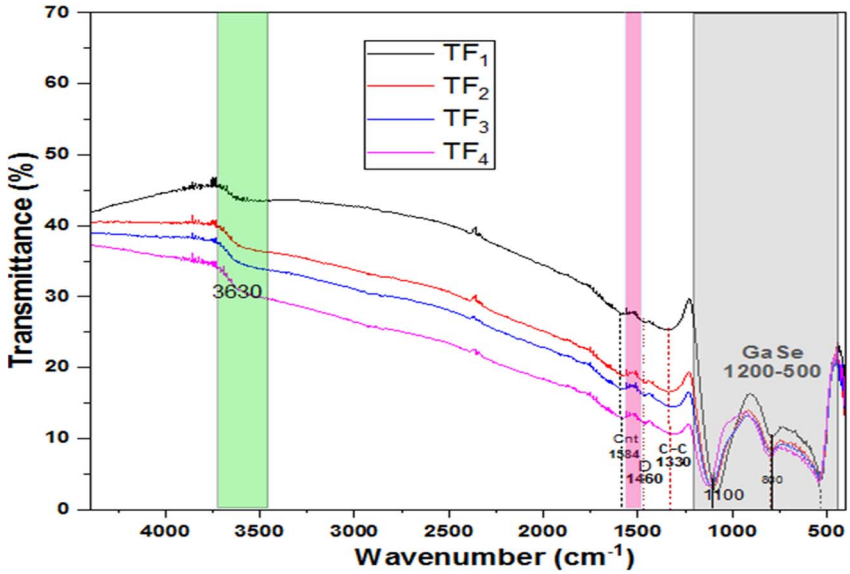


Fig. 2 FTIR spectra of the as-prepared and SHI-irradiated thin films of $(Ga_{10}Se_{90})$-CNT.

order vibrational modes of Ga-Se. This could also reflect the interlayer coupling in $Ga_{10}Se_{90}$ involving both in-plane and out-of-plane vibrations. The low intensity broad peak around 800 $cm^{-1}$ is attributed to bonding of $Ga_{10}Se_{90}$ with MWCNTs. The small peak at 1460 $cm^{-1}$ is attributed to the D band peak of MWCNTs, and it may be due to the defects induced in the crystal due to SHI irradiation. The small peak at 1584 $cm^{-1}$ is attributed to C–C stretching of CNTs, which is obviously due to the incorporation of CNTs. The small extra peaks around 1500 $cm^{-1}$ are attributed to C–C bonding and defects of MWCNTs.[26,27] The less intense peaks of CNTs found in the spectra may be due to low concentration of CNTs compared to $Ga_{10}Se_{90}$. Thus, FTIR studies confirm the incorporation of CNTs with $Ga_{10}Se_{90}$ particles, which could lead to enhancement of the mechanical strength and thermal stability of the as-prepared thin films of $(Ga_{10}Se_{90})$-MWCNT. The small wide lump like peak around 3630 $cm^{-1}$ may be attributed to O–H stretching, which may be due to the solvent used or defects created in the material.

### 3.3 Electrical properties

The variations of dark DC current ($I_{DC}$) with applied voltage in the range of 0.2 to 4 eV of the as-prepared bilayer and swift heavy ion irradiated thin films of $(Ga_{10}Se_{90})$-CNT are shown in Fig. 3(a). Straight lines are obtained, indicating that these films all exhibit ohmic behavior. The photocurrent *versus* applied voltage shows a similar kind of behavior as the DC current (see Fig. 3(b)). From these plots, it is clearly found that both the dark DC current and photo-current increase with increasing fluence

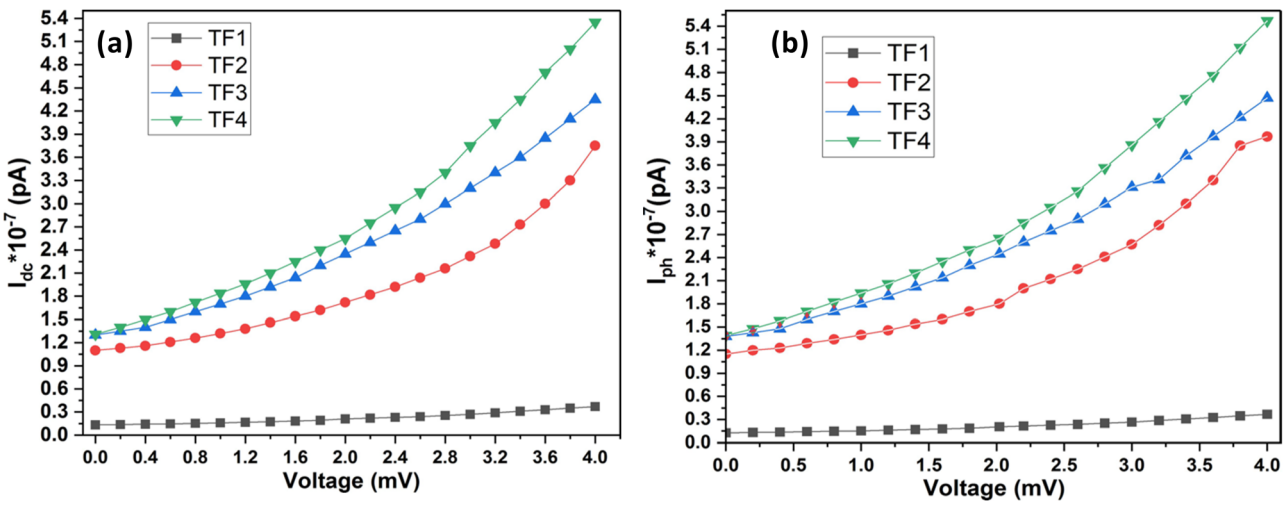


Fig. 3 Variations of the dark DC current and photocurrent with the applied voltage. (a) Dark DC current *versus* voltage, and (b) photocurrent *versus* voltage of the as-prepared and SHI-irradiated thin films of $(Ga_{10}Se_{90})$-CNT.

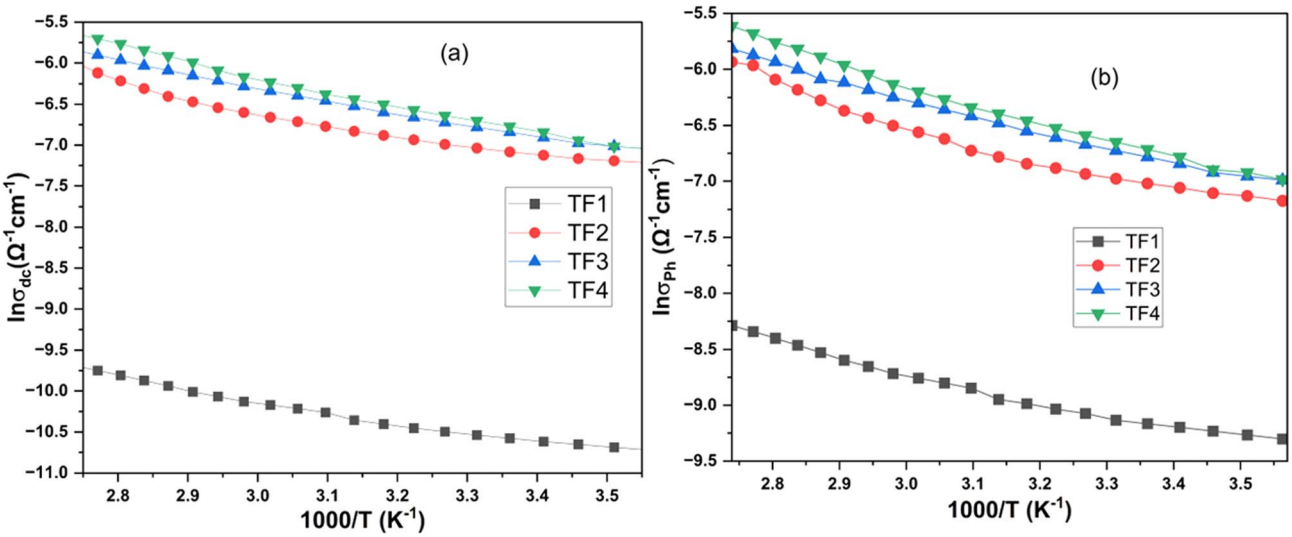


Fig. 4 DC conductivity and photoconductivity of the as-prepared (un-irradiated) and SHI-irradiated thin films of the $(Ga_{10}Se_{90})$-CNT composite. (a) DC conductivity: variation of $\ln(\sigma_{DC})$ *vs.* $1000/T$. (b) Photoconductivity: variation of $\ln(\sigma_{ph})$ *vs.* $1000/T$.

of SHI irradiation, which is obviously due to the presence of highly conductive CNT nanotubes. The conductivity measurements were evaluated in the temperature range of 293.32 K to 365.09 K at a constant voltage of 1.5 V (for accurate measurements). The conductivity mainly depends on the mobility of charge carriers. The greater the mobility of the charge carriers, the greater the conductivity. CNTs are nanotubes with diameters of the order of a few nanometers and lengths that can range from the nm to cm range, thus providing direct pathways for charge carrier transportation, resulting in increased mobility of charge carriers and correspondingly increased conductivity. Conductivity also depends on the density of charge carriers, and the greater the density of charge carriers, the greater the conductivity. The variation of DC conductivity of the as-prepared and SHI-irradiated thin films of $(Ga_{10}Se_{90})$-CNT with temperature is plotted according to the Arrhenius equation as shown in Fig. 4(a). The Arrhenius equation is as follows:

$$\sigma_{DC} = \sigma_0 \exp[-\Delta E_{DC}/KT] \quad (1)$$

where $\sigma_0$ is the pre-exponential factor, and $K$ = Boltzmann constant = $8.6\,173\,303/10^{-5}$ eV $K^{-1}$. $\ln \sigma_{DC}$ *vs.* $1000/T$ is plotted in the temperature range of 279 K to 393 K, as shown in Fig. 4(a). Straight lines are obtained, indicating that the conduction occurs through an activated process. From this analysis, it is found that the DC conductivity increases (of the order of 8.6 $\Omega^{-1}$ $cm^{-1}$) with increasing ion fluence, as the conductivity curves of SHI-irradiated thin films lie above that of the unexposed (as-prepared) thin film (see Fig. 3). The slope of $\ln(\sigma)$ *vs.* $1000/T$ gives the activation energy, as is given by the formula:

$$\ln(\sigma) = \ln(\sigma_0) - \Delta E/KT \quad (2)$$

The parameter values obtained are tabulated in Table 1, showing that the value of the activation energy decreases with

Table 1 DC conductivity parameters at a temperature of 352.4 K of the as-prepared and SHI-irradiated thin films of $(Ga_{10}Se_{90})$-CNT

| Sample | $\sigma_{DC}$ ($\Omega^{-1}$ $cm^{-1}$) | $(E_a)_{DC}$ (eV) | $(\sigma_0)_{DC}$ ($\Omega^{-1}$ $cm^{-1}$) |
|---|---|---|---|
| TF1 | $2.11 \times 10^{-4}$ | $4.25 \times 10^{-4}$ | $2.14 \times 10^{-4}$ |
| TF2 | $2.07 \times 10^{-3}$ | $1.65 \times 10^{-4}$ | $2.08 \times 10^{-3}$ |
| TF3 | $2.48 \times 10^{-3}$ | $1.62 \times 10^{-4}$ | $2.49 \times 10^{-3}$ |
| TF4 | $2.97 \times 10^{-3}$ | $1.39 \times 10^{-4}$ | $2.99 \times 10^{-3}$ |

increasing ion fluence of swift heavy ion irradiation. The variation of photoconductivity of the as-prepared thin films with temperature (Fig. 4(b)) is plotted according to the same Arrhenius equation used for DC conductivity measurements.

$$\sigma_{Ph} = \sigma_0 \exp[-\Delta E_{Ph}/KT] \quad (3)$$

The photoconductivity measurements displayed a similar kind of behavior to the DC conductivity. From Fig. 4(b), $\ln(\sigma_{Ph})$ *vs.* $1000/T$ in the same temperature range of 279 K to 393 K is plotted, and again straight lines are obtained indicating the ohmic behavior, and it is found that the photoconductivity increases with increasing fluence of SHI irradiation, while the activation energy decreases. The $Ga_{10}Se_{90}$ particle size decreases after swift heavy ion irradiation leading to quantum confinement effects, thus decreasing the scattering mechanisms, hence increasing the exciton mobility. The measured DC conductivity and photoconductivity parameters of the as-prepared (un-irradiated) and SHI-irradiated thin films at a temperature of 352.4 K are shown in Tables 1 and 2, respectively. From Table 1, it is found that the dark-DC conductivity of the SHI-irradiated thin films increased by a magnitude of the order of 8.567 ($\Omega^{-1}$ $cm^{-1}$) compared to the as-prepared (un-irradiated) thin film TF1. Similarly, from Table 2, it is found that the photoconductivity of the SHI-irradiated TF4 thin film with high

Table 2 Photoconductivity parameters at a temperature of 352.4 K of the as-prepared and SHI-irradiated thin films of ($Ga_{10}Se_{90}$)-CNT

| Sample | $\sigma_{Ph}$ ($\Omega^{-1}$ cm$^{-1}$) | $(E_a)_{Ph}$ (eV) | $(\sigma_0)_{Ph}$ ($\Omega^{-1}$ cm$^{-1}$) |
|---|---|---|---|
| TF1 | $5.16 \times 10^{-5}$ | −9.8707 | $5.18 \times 10^{-5}$ |
| TF2 | $1.82 \times 10^{-3}$ | −6.30892 | $1.82 \times 10^{-3}$ |
| TF3 | $2.40 \times 10^{-3}$ | −6.03229 | $2.39 \times 10^{-3}$ |
| TF4 | $2.90 \times 10^{-3}$ | −5.84304 | $2.39 \times 10^{-3}$ |

fluence also increased by a remarkable magnitude of the order of 226.67 ($\Omega^{-1}$ cm$^{-1}$) compared to the un-irradiated TF1 thin film.

The homogeneous mixing of the bi-layered $Ga_{10}Se_{90}$-MWCNT composite by SHI irradiation resulted from the decreased particle size of GaSe that advantages optoelectronic device fabrications. The quantum confinement leads to a decrease of scattering mechanisms, resulting in increasing exciton mobility. The dark DC conductivity and photoconductivity increase, while the activation energy decreases with increasing fluence of SHI irradiation. The conductivity measurements displayed a considerable improvement in terms of the dark DC conductivity and photoconductivity of the SHI-irradiated bilayer thin films compared to the as-prepared thin film. The dark DC conductivity increased notably by a magnitude of the order of 8.6 ($\Omega^{-1}$ cm$^{-1}$), post SHI irradiation. The photoconductivity also increased significantly by a magnitude of the order of 226.67 ($\Omega^{-1}$ cm$^{-1}$), post SHI irradiation. This enhancement found in the conductivity values is obviously due to the high electrical conductivity and high mobility of the CNT nanotubes. The enhanced DC conductivity and photoconductivity of the investigated composite material suggest its potential opto-electronic device applications.

### 3.4 Mobility

The mobility of the as-prepared and SHI-irradiated thin films is estimated with the help of the well-known Hall effect technique (van der Pauw's method). This measurement was carried out at a room temperature (*i.e.* 300 K) and at a magnetic field intensity of 0.570 Tesla. The Hall measurement analysis of the investigated thin films displayed a remarkable change in mobility after SHI irradiation (see Table 3). The mobility parameters of the as-prepared and SHI-irradiated thin films are shown in Table 3. The Hall coefficient of the as-prepared bi-layer thin film TF1 has a negative sign, indicating that the electrons are majority carriers, and hence contribute to any conduction processes. However, the Hall coefficient of SHI-irradiated thin films has a positive sign, revealing that the holes are responsible for conduction processes in these thin films. This also indicates that the as-prepared thin film shows n-type semiconducting behavior. Meanwhile, due to homogeneous mixing of $Ga_{10}Se_{90}$ with MWCNTs after exposure to SHI irradiation, the behavior completely changed from n-type to p-type, and thus holes contributed to any conduction. The mobility of the as-prepared thin film TF1 of ($Ga_{10}Se_{90}$)-MWCNT at a magnetic field of 0.570 T at room temperature is found to be 50.99 cm$^2$ V$^{-1}$ s$^{-1}$, while the mobility values increased appreciably upon SHI irradiation. The estimated mobility values of the SHI-irradiated thin films TF2, TF3, and TF4 at a magnetic field of 0.570 T at room temperature, 300 K, are found to be 274.4 cm$^2$ V$^{-1}$ s$^{-1}$, 343.1 cm$^2$ V$^{-1}$ s$^{-1}$ and 475.1 cm$^2$ V$^{-1}$ s$^{-1}$, respectively. The variation of mobility with the fluence 70 MeV $Ni^+$ ions is depicted graphically in Fig. 5. From Fig. 5, it is clearly seen that the mobility increased upon SHI irradiation. This is due to the homogeneous mixing of MWCNTs into the thermally evaporated $Ga_{10}Se_{90}$ and the reducing size of $Ga_{10}Se_{90}$ nanoparticles upon SHI irradiation, which resulted in the release of trapped exciton pairs, which are free to move to contribute to the conduction of the crystal. This remarkable increase in the mobility values is promising for applications, making this material a possible candidate for various optoelectronic applications.

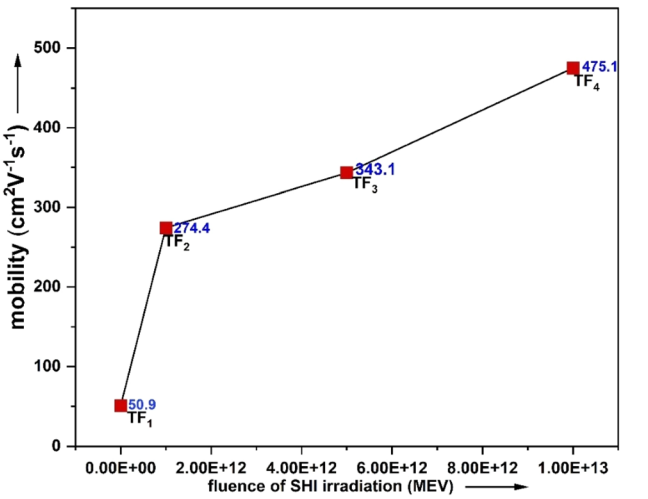


Fig. 5 Variation of mobility ($\mu$) with SHI irradiation. TF1 is the unirradiated thin film, while TF2, TF3 and TF4 are SHI-irradiated thin films of the $Ga_{10}Se_{90}$-MWCNT composite at fluences of $1 \times 10^{12}$, $1 \times 10^{12}$ and $1 \times 10^{13}$ ions per cm$^2$, respectively.

Table 3 Mobility ($\mu$) studies of as-prepared and SHI-irradiated thin films of ($Ga_{10}Se_{90}$)-CNT at a magnetic field intensity of 0.570 T at room temperature (300 K), using the Hall effect

| S. no | $I$ (A) | $R_H$ (cm$^{-3}$ C$^{-1}$) | $N$ (cm$^{-3}$) | $P$ ($\Omega$ cm$^{-1}$) | $\sigma$ ($\Omega^{-1}$ cm$^{-1}$) | $\mu$ (cm$^2$ V$^{-1}$ s$^{-1}$) |
|---|---|---|---|---|---|---|
| TF1 | 0.050 | $-9.79 \times 10^4$ | $-6.37 \times 10^{14}$ | $1.92 \times 10^3$ | $5.19 \times 10^{-4}$ | $5.09 \times 10^1$ |
| TF2 | 0.010 | $1.20 \times 10^6$ | $5.19 \times 10^{12}$ | $3.31 \times 10^3$ | $2.28 \times 10^{-4}$ | $2.74 \times 10^2$ |
| TF3 | 0.020 | $1.72 \times 10^5$ | $3.62 \times 10^{13}$ | $5.02 \times 10^2$ | $1.98 \times 10^{-3}$ | $3.43 \times 10^2$ |
| TF4 | 0.040 | $3.46 \times 10^6$ | $1.80 \times 10^{13}$ | $3.24 \times 10^2$ | $0.13 \times 10^{-3}$ | $0.47 \times 10^3$ |

## 4. Conclusions

This work studies the effect of the incorporation of MWCNTs on the opto-electronic properties of $Ga_{10}Se_{90}$ bilayer thin films. SHI irradiation of 70 MeV $Ni^{7+}$ ions in a fluence range of $1 \times 10^{12}$ to $1 \times 10^{13}$ ions per $cm^2$ is employed for the uniform distribution of CNTs into GaSe matrix layers, for modification of the electrical properties. This study shows a remarkable enhancement in conductivity values of $Ga_{10}Se_{90}$-MWCNT composite thin films after SHI irradiation. The DC conductivity of $(Ga_{10}Se_{90})$-MWCNT increased by 8.6 $\Omega^{-1}$ $cm^{-1}$ upon SHI irradiation compared to the as-prepared (un-irradiated) thin film. The photoconductivity also increased by a remarkable 226.67 $\Omega^{-1}$ $cm^{-1}$ upon SHI irradiation compared to the as-prepared thin film. From mobility studies, it is clearly found that the mobility of the SHI-irradiated TF4 thin film of $(Ga_{10}Se_{90})$-MWCNT increased from 50.9 $cm^2$ $V^{-1}$ $s^{-1}$ (TF1) to 475.1 $cm^2$ $V^{-1}$ $s^{-1}$ (TF4), by 424.2 $cm^2$ $V^{-1}$ $s^{-1}$, making it a potential candidate for various photoelectric applications. EDX analysis confirmed the elemental composition. Surface studies clearly showed the incorporation of Ga-Se nanoparticles into the matrix layers of CNTs. FTIR analysis showed intense peaks of GaSe nanoparticles and CNTs, confirming the uniform distribution of CNTs into the GaSe matrix layers. Electrical measurements showed the increased dark DC conductivity and photoconductivity of the SHI-irradiated thin films. The enhanced conductivity and mobility values are very important, considering the potential applications. The very large ranges found in the conductivity and mobility make the investigated material a possible candidate for various optoelectronic applications, such as in photodetectors, photodiodes, photoconductors, *etc.* The fabricated thin-film composite material $Ga_{10}Se_{90}$-MWCNT, due to its novel electrical properties, can be integrated into various opto-electronic devices, such as photoconductors, photodetectors, printers, *etc.*

## Conflicts of interest

The authors declare the following financial interests/personal relationships which may be considered as potential competing interests.

## Data availability

All data generated or analysed during this study are included in the published article.

## Acknowledgements

The authors express their sincere gratitude to Prof. M. Zulfequar, Department of Physics, Jamia Millia Islamia, New Delhi, India, for his valuable discussions and laboratory support. We gratefully acknowledge the Inter-University Accelerator Centre (IUAC), New Delhi, for providing the beam time facility utilized in this study. Financial assistance from the J&K State Council for Science and Technology (JKSTIC/SRE/946-50) is also duly acknowledged.

## References

1 V. Chitra, S. Vasantha and K. R. Murali, Structural, optical, electrical and photoconducting properties of pulse plated Copper Gallium selenide films, *Compos. Part B Eng.*, 2014, **58**, 160–165, DOI: 10.1016/j.compositesb.2013.10.046.
2 S. Hudgens and B. Johnson, Overview of Phase-Change Chalcogenide Nonvolatile Memory Technology, *MRS Bull.*, 2004, **29**(11), 829–832, DOI: 10.1557/mrs2004.236.
3 S. Ruzgar, The effect of strontium doping on optoelectrical properties of V2O5/p-Si photodiode, *Opt. Mater.*, 2024, **157**, 116087, DOI: 10.1016/j.optmat.2024.116087.
4 Ş. Rüzgar and V. Eratilla, The Effect of Deposition Temperature on Structural, Morphological, and Dielectric Properties of Yttria-Doped Zirconia Thin Films, *Sinop Üniv. fen bilim. derg.*, 2024, **9**(1), 44–60, DOI: 10.33484/sinopfbd.1369460.
5 X. Li, *et al.*, Controlled Vapor Phase Growth of Single Crystalline, Two-Dimensional GaSe Crystals with High Photoresponse, *Sci. Rep.*, 2014, **4**(1), 5497, DOI: 10.1038/srep05497.
6 L. Tan, *et al.*, Effective shape-controlled synthesis of gallium selenide nanosheets by vapor phase deposition, *Nano Res.*, 2020, **13**(2), 557–563, DOI: 10.1007/s12274-020-2653-8.
7 C. S. Jung, *et al.*, Red-to-Ultraviolet Emission Tuning of Two-Dimensional Gallium Sulfide/Selenide, *ACS Nano*, 2015, **9**(10), 9585–9593, DOI: 10.1021/acsnano.5b04876.
8 E. Zhu, C. Lin, Q. Jiao, B. Song, X. Liu and S. Dai, Effect of gallium addition on physical and structural properties of Ge–S chalcogenide glasses, *Ceram. Int.*, 2017, **43**(15), 12205–12208, DOI: 10.1016/j.ceramint.2017.06.080.
9 X. Li, *et al.*, Revealing the Preferred Interlayer Orientations and Stackings of Two-Dimensional Bilayer Gallium Selenide Crystals, *Angew. Chem. Int. Ed.*, 2015, **54**(9), 9, DOI: 10.1002/anie.201409743.
10 B. Shevitski, *et al.*, Tunable electronic structure in gallium chalcogenide van der Waals compounds, *Phys. Rev. B*, 2019, **100**(16), 165112, DOI: 10.1103/PhysRevB.100.165112.
11 M. Di Giulio, G. Micocci, P. Siciliano and A. Tepore, Photoelectronic and optical properties of amorphous gallium-selenide thin films, *J. Appl. Phys.*, 1987, **62**(10), 4231–4235, DOI: 10.1063/1.339095.
12 N. C. Fernelius, Properties of gallium selenide single crystal, *Prog. Cryst. Growth Charact. Mater.*, 1994, **28**(4), 275–353, DOI: 10.1016/0960-8974(94)90010-8.
13 S. Lei, *et al.*, Synthesis and Photoresponse of Large GaSe Atomic Layers, *Nano Lett.*, 2013, **13**(6), 2777–2781, DOI: 10.1021/nl4010089.
14 L. Karvonen, *et al.*, Investigation of Second- and Third-Harmonic Generation in Few-Layer Gallium Selenide by Multiphoton Microscopy, *Sci. Rep.*, 2015, **5**(1), 10334, DOI: 10.1038/srep10334.
15 H. Arora and A. Erbe, Recent progress in contact, mobility, and encapsulation engineering of InSe and GaSe, *InfoMat*, 2021, **3**(6), 662–693, DOI: 10.1002/inf2.12160.

16 T. Demirtaş, C. Odacı and U. Aydemir, Enhanced photoresponse of PVP:GaSe nanocomposite thin film based photodetectors, *Nanotechnology*, 2022, **33**(20), 205506, DOI: **10.1088/1361-6528/ac5284**.

17 N. Tohge, H. Matsuo and T. Minami, Electrical properties of n-type semiconducting chalcogenide glasses in the system Pb-Ge-Se, *J. Non-Cryst. Solids*, 1987, **95**(96), 809–816, DOI: **10.1016/S0022-3093(87)80685-3**.

18 S. Kumar Yadav, A. Kumar and N. Mehta, Tailoring of physical properties of glassy selenium (g-Se) by using multi-walled carbon nanotubes (MWCNTs), *Mater. Sci. Eng. B*, 2023, **290**, 116310, DOI: **10.1016/j.mseb.2023.116310**.

19 P. Jaiswal and D. K. Dwivedi, Effect of CNT on thermal properties and temperature dependent electrical properties of Cu-Se-Ge-In chalcogenide glasses, *Mater. Res. Express*, 2019, **6**(5), 055203, DOI: **10.1088/2053-1591/ab063d**.

20 M. Ganaie and M. Zulfequar, Structural, electrical and dielectric properties of CNT doped SeTe glassy alloys, *Mater. Chem. Phys.*, 2016, **177**, 455–462, DOI: **10.1016/j.matchemphys.2016.04.053**.

21 S. Ahmad, M. Singh, M. Zulfequar, J. Ali and A. Kandasami, Ion Beam-Induced Modification in the Optical Properties of the Bilayer of Nano-Structured Amorphous Selenium and Multi-Walled Carbon Nanotubes: A Study by 70 Mev Ni Ion Irradiation, *Mater. Lett.*, 2024, **371**, 136878, DOI: **10.2139/ssrn.4766383**.

22 E. M. Bringa and R. E. Johnson, Coulomb Explosion and Thermal Spikes, *Phys. Rev. Lett.*, 2002, **88**(16), 165501, DOI: **10.1103/PhysRevLett.88.165501**.

23 M. Abushad, *et al.*, Swift heavy ion irradiation induced modifications on the structure, optical and electrical properties of pulsed laser deposited anatase TiO2 thin films, *Radiat. Phys. Chem.*, 2024, **216**, 111371, DOI: **10.1016/j.radphyschem.2023.111371**.

24 Z. H. Khan, S. A. Khan, N. Salah, S. Habib, S. M. Abdallah El-Hamidy and A. A. Al-Ghamdi, Effect of Composition on Electrical and Optical Properties of Thin Films of Amorphous Ga x Se100−x Nanorods, *Nanoscale Res. Lett.*, 2010, **5**(9), 1512–1517, DOI: **10.1007/s11671-010-9671-5**.

25 H. Khan, Z. M. S. H. Khan, S. Islam, R. S. Rahman, M. Husain and M. Zulfequar, Electrical properties of carbon nanotubes modified GaSe glassy system, *AIP Conference Proceedings*, AIP Publishing, 2018, vol. 1953, p. 090065, DOI: **10.1063/1.5032912**.

26 W. Lin, Y. Xiu, L. Zhu, K.-S. Moon, and C. P. Wong, "Assembling of carbon nanotube structures by chemical anchoring for packaging applications," in *2008 58th Electronic Components and Technology Conference, Lake Buena Vista, FL, USA: IEEE*, 2008, pp. 421–426, DOI: **10.1109/ECTC.2008.4550005**.

27 B. Singh, D. Singh, R. Mathur and T. Dhami, Influence of Surface Modified MWCNTs on the Mechanical, Electrical and Thermal Properties of Polyimide Nanocomposites, *Nanoscale Res. Lett.*, 2008, **3**(11), 444, DOI: **10.1007/s11671-008-9179-4**.